Computational Studies on Realkylation Reactions of Aged-Acetylcholinesterase with Quinone Methide Precursors for Regenerating Nerve Agent Aged Acetylcholinesterase

by

Ian M. Pelfrey

The Ohio State University
April 2018

The Ohio State University Department of Chemistry and Biochemistry, Columbus OH, 43210

Project Advisor: Dr. Ryan Yoder

Abstract

Organophosphorus compounds (OPs) such as sarin, soman, and tabun are toxic nerve agents used in chemical warfare and as pesticides. These OPs covalently bond with Ser_{203}, a catalytic residue in the enzyme acetylcholinesterase (AChE), preventing hydrolysis of the neurotransmitter acetylcholine into acetate and choline. Once exposed to an OP compound, the inhibited AChE will undergo an irreversible process known as aging, where the OP-AChE complex will dealkylate and form a stable phosphonate anion on the Ser_{203} residue, inactivating the enzyme. Without functioning AChE, acetylcholine accumulates in the central nervous system causing seizures, vomiting, and often death. Currently, there are no known therapeutic methods to reverse this aging process to regain enzymatic activity.

However, inhibited AChE can be restored to the active AChE before the onset of the aging process by treatment with pharmaceuticals containing an oxime functional group. The goal of this project is to discover a compound that will realkylate the phosphonate group on the Ser_{203} in aged-AChE, which can then be restored to the active AChE by oxime treatment. Literature shows that quinone methides (QMs) are capable of alkylating phosphodiesters, which are structurally similar to the phosphylated Ser_{203} residue in the aged-AChE active site. Through computational methods (molecular docking, molecular dynamics, and tomodock), potential poses in AChE of a variety of quinone methide precursors (QMPs) were analyzed *in silico* to determine their putative efficacy *in vitro*.

Acknowledgements

I would like to acknowledge the people who made this thesis possible. I want to thank Dr. Ryan Yoder for being a patient and inspiring mentor, I'm so glad we were able to work together. I also want to thank Nathan Yoshino and Rachel Hopper for their help and friendship while we worked on parts of this project. Also Dr. Christopher Callam for introducing me to Dr. Yoder when I approached him with the idea of doing research, and Dr. Christopher Hadad, without whose leadership the whole project wouldn't be possible.

Contents

1. Introduction

1.1 Quinine Methide Precursors as Potential Therapeutics for OP Exposure

Organophosphorus compounds (OPs), also known as phosphate esters, find use primarily as insecticides, herbicides, and chemical warfare agents. They are classified as some of the most toxic compounds ever developed due to their ability to cause fatal poisonings in sub-milligram dosages [1]. After characterization of OPs in 1932 by German scientist Willy Lange they were adapted for industrial use in the 1930s by another German scientist, Gerhard Schrader [2]. He created the first OP, tabun, as a pesticide and at the behest of the German government he created the first OP nerve agents, sarin and soman. (Figure 1) OPs have been used as weapons of war in Syria and Iraq as well as terrorist weapons in the Tokyo subway attack [3],[4]. Combined with accidental OP insecticide exposure thousands of people are hurt by OP compounds every year. Many OPs are now classified as weapons of mass destruction by the United Nations [5] and have been a threat since the 1990s because of their ease of synthesis and acute toxicity. Because OPs are an ongoing threat with limited treatment potential new treatment techniques need investigation.

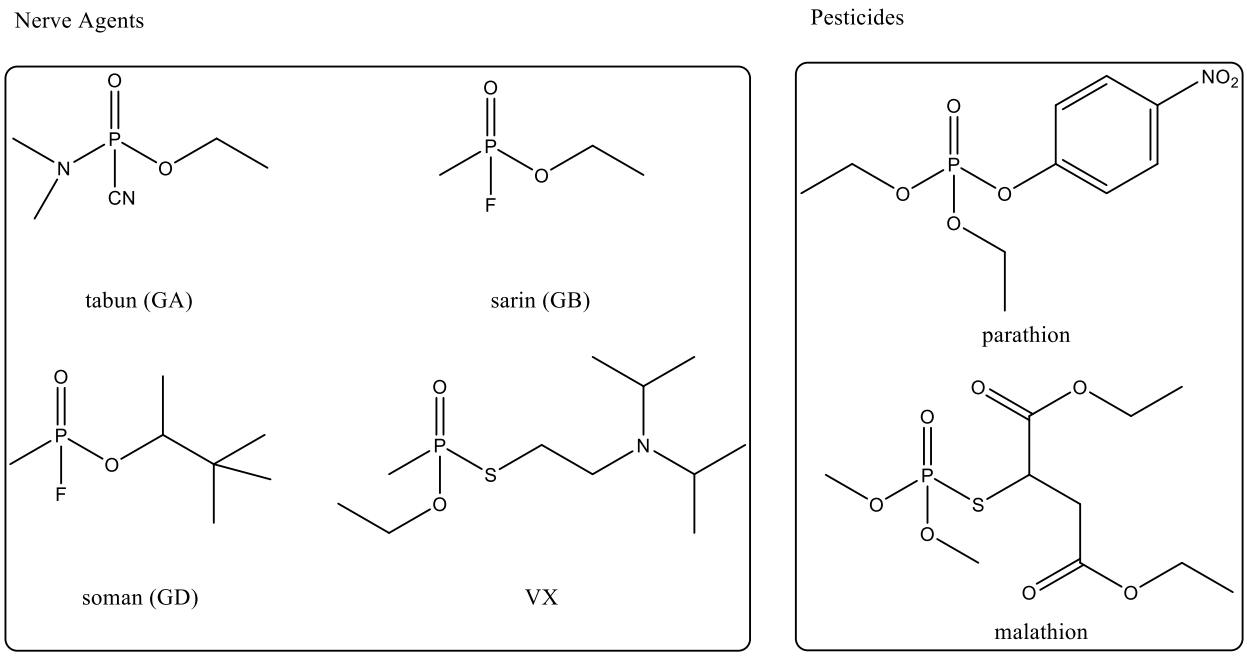

Figure 1.1: Structures of OP nerve agents and insecticides

OPs exert their toxic effect by inhibiting the enzyme acetylcholinesterase (AChE). This enzyme hydrolyzes the neurotransmitter acetylcholine (ACh) into choline and acetate by binding ACh to the Ser_{203} residue of the catalytic triad in the active site. (Figure 1.2) ACh is responsible for muscle activation and contraction as well as memory and arousal [6]. AChE serves to attenuate the ACh signal so nerve signals stop and the muscles can relax [6]. When the OP enters the active site of AChE the phosphonate binds the active serine residue of the enzyme's' catalytic triad. (Figure 1.2) In this form with the OP bound the enzyme is inhibited and unable to act on ACh. Once the OP is bound to Ser_{203} it undergoes a secondary reaction within several minutes to hours called aging. The aging process is when the bound OP is dealkylated, and the alkyl component leaves the active site of AChE, however, the phosphonate group remains bound to Ser_{203} permanently inhibiting the enzyme.

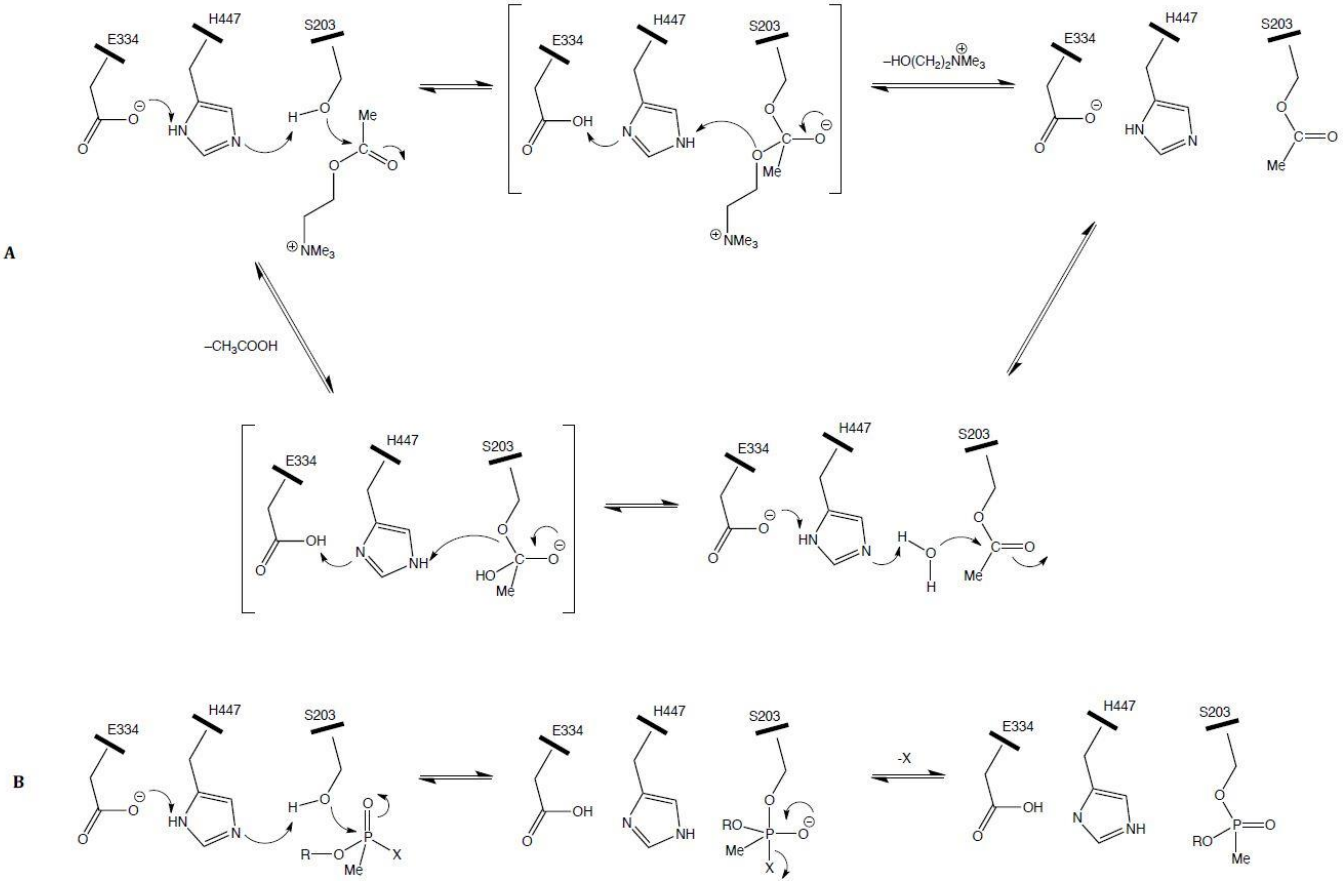

Figure 1.2: (**A**) AChE uses Serine-Histidine-Glutamate catalytic triad to hydrolyze AChE to acetate and choline. (**B**) OP inhibition of AChE due to P-O covalent bond.

Before the aging process takes place, the inhibited enzyme can be regenerated into functioning AChE with administration of reactive oxime drugs which will reverse phosphylation. However, oximes are ineffective for treatment of the aged complex. The aged AChE results in a rapid buildup of ACh in neuromuscular synapses causing hyperarousal and extreme muscle contraction. Acute OP poisoning symptoms present as convulsions, paralysis, and death via asphyxiation. The window for treatment of OP poisoning is very short and depending on the size of the alkyl chain of the OP in question oxime treatment may not be adequate to reverse enough AChE prior to aging [12].

Preliminary Studies

Quinone methide precursors (QMPs) are high energy reactive biological electrophiles that are thought to be powerful alkylating agents. (Figure 1.3) [7] QMPs have also been shown to participate in DNA-alkylation and previous research into the alkylation activity of their isomers and derivatives is available [8].

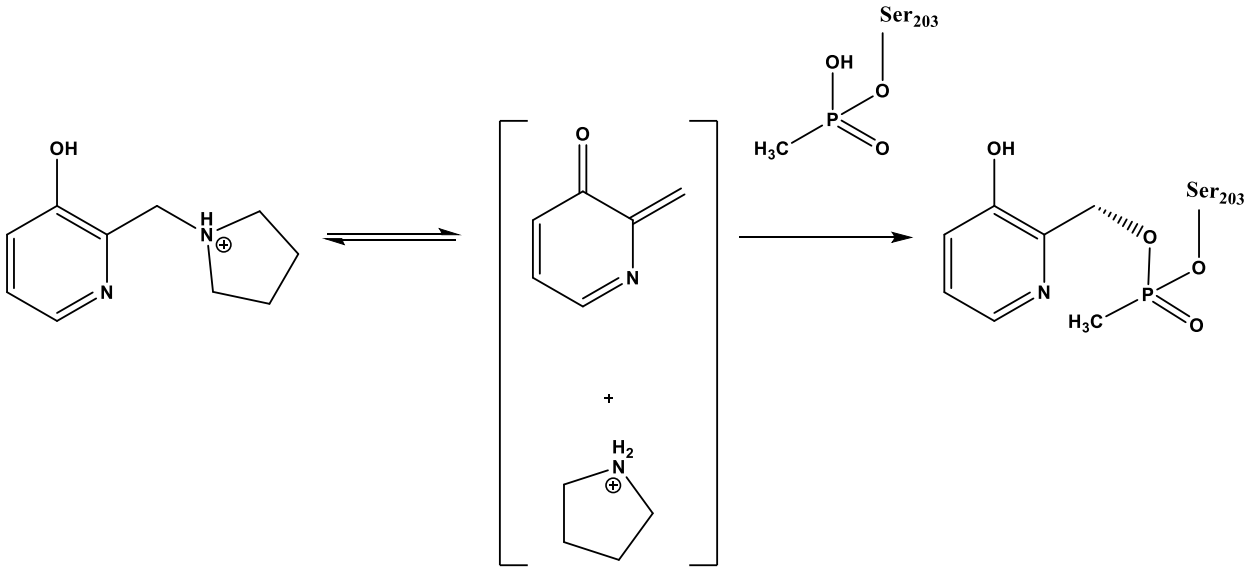

Figure 1.3: Proposed pyridine based quinone methide precursor alkylation reaction. The reactive intermediate, once generated in the active site will be able to bind the phosphonate oxygen, realkylating it and preparing the complex for oxime treatment.

Of specific interest is a study by Bakke et al. which shows ortho- QMPs possess the ability to alkylate phosphodiester [9]. This is important because it suggests that QMPs possess the ability to realkylate aged AChE and make it susceptible to treatment with oxime-type drugs.

1.2 References

[1] Lewis, Robert Alan (1998). *Lewis' Dictionary of Toxicology*. CRC Lewis. p. 763. ISBN 978-1-56670-223-2. Retrieved 18 July 2013.

[2] Paxman, J.; Harris, R. *A Higher Form of Killing: The Secret Story of Chemical and Biological Warfare*, Hill and Wang: New York, 1982: pp 53-67,138-139

[3] *Amy E. Smithson and Leslie-Anne Levy (October 2000). "Chapter 3 – Rethinking the Lessons of Tokyo". Ataxia: The Chemical and Biological Terrorism Threat and the US Response (Report). Henry L. Stimson Centre. pp. 91,95,100. Report No. 35. Retrieved 15 December 2014*

[4] Human Rights Watch, *Iraq's Crime Of Genocide: The Anfal Campaign against the Kurds* (Human Rights Watch, 1994), http://www.hrw.org/reports/1994/05/01/iraq-s-crime-genocideanfal-campaign-against-kurds.

[5] Security Council Resolution 687, S/RES/687 (8 April 1991) available from www.un.org/Depts/unmovic/documents/687.pdf

[6] Jones, BE (2005). "From waking to sleeping: neuronal and chemical substrates". *Trends in pharmacological sciences*. 26 (11): 578–86. doi:10.1016/j.tips.2005.09.009. PMID 16183137.

[7] Veldhuyen, W.F.; Shallop, A. J.; Jones, R. A.; Rokita, S. E. *J. Am. Chem. Soc.* 2001, *123,* 11126.

[8] Modica, E.; Zanaletti, R.; Freccero, M.; Mela,M. *J. Org. Chem.* 2001, 66, 41

[9] Bakke, B. A.; McIntosh, M. C.; Turnbull, K. D. *J. Org. Chem.* 2005, 70, 4338-4345

[10] Michel, H. O., Hackley, B. E. Jr, Berkowitz, L., List, G., Hackley, E. B., Gilliam, W. and Paukan, M. (1967) Aging and dealkylation of soman (pinocolylmethyl-phosphonofluoridate)-Inactivated eel cholinesterase. Arch. Biochem. Biophys. 121, 29-34.

[11] Ballantyne, B. and Marrs, T. C. (1992). Overview of the biological and clinical aspects of organophosphates and carbamates, in Clinical and Experimental Toxicology of Organophosphates and Carbamates, Ballantyne, B. and Marrs, T. C., Eds., Butterworth, Oxford, England, 1.

[12] Dacre, J. C. (1984). Toxicology of some Anticholinesterases used as chemical warfare agents - a review, in Cholinesterases, Fundamental and Applied Aspects, Brzin, M., Barnard, E. A. and Sket, D., Eds., de Gruyter, Berlin, Germany, 415.

[13] Rogin, J. Exclusive: U.S. to Bring Chemical Weapons Witnesses Out of Syria. *The Daily Beast*, May 2013, http://www.thedailybeast.com/articles/2013/05/22/exclusive-u-s-to-bringchemical-weapons-witnesses-out-of-syria.html (accessed May 27, 2013).

[14] Médecins Sans Frontières, "Syria: Thousands Suffering from Neurotoxic Symptoms Treated in Hospitals Supported by MSF," August 24, 2013.

[15] Seto, Dr. Yasuo: The Sarin Gas Attack in Japan and the Related Forensic Investigation. Org. for Prohibition of Chemical Weapons, June 2001, http://www.opcw.org/news/article/the-saringas-attack-in-japan-and-the-related-forensic-investigation/ (accessed September 16th, 2014)

[16] Worek, F., Szinicz, L., Eyer, P. and Thiermann, H. (2005) Evalulation of oxime efficacy in nerve agent poisoning: Development of a kinetic-based dynamic model, Toxicol. Appl. Pharmacol. 209, 193-202.

2. Initial Library

2.1 Introduction

A library of 39 quinone methide precursors (QMPs) for computational analysis was decided upon with collaborators. These compounds we based off the lead compound corriganine. (Figures 2.1) We modified the lead compound to contain electron withdrawing and electron donating substituents at the positions R_4, R_5 and R_6. (Figures 2.1- 2.4)

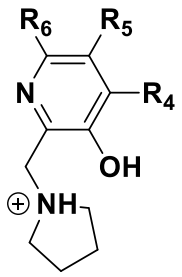

Figure 2.1: Corriganine scaffold with labeled substituent positions.

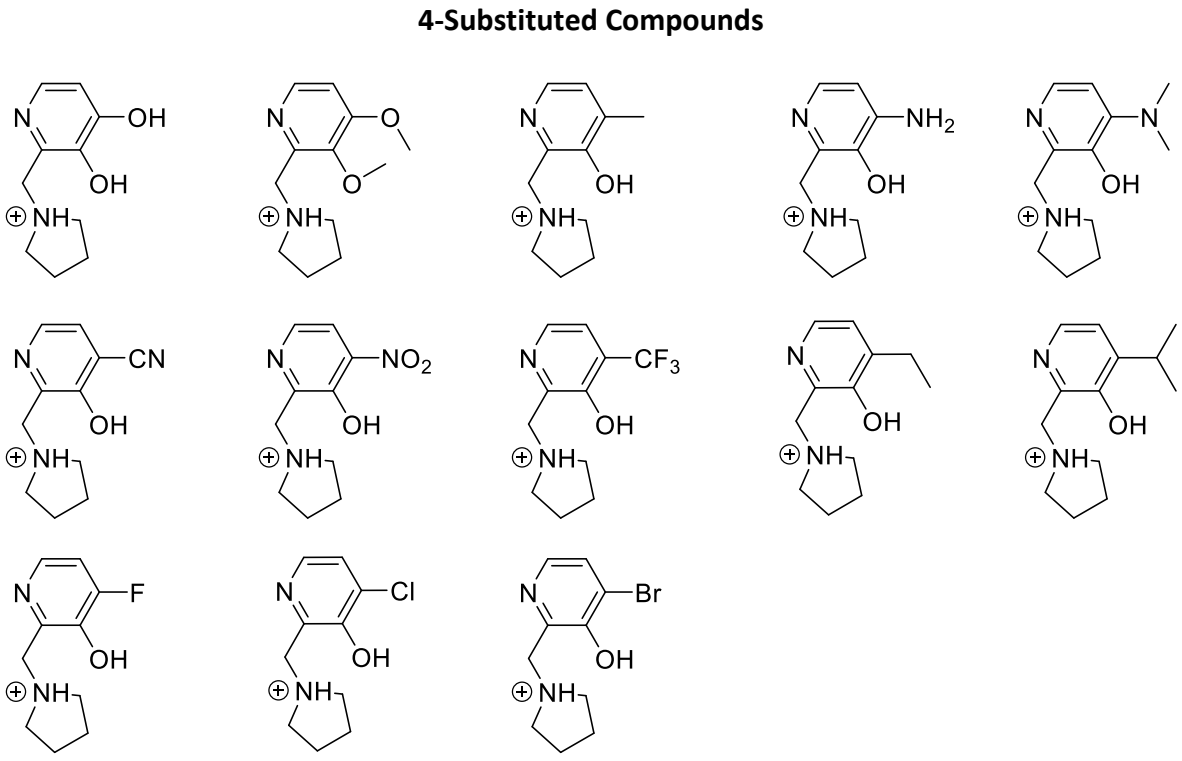

Figure 2.2: Library of quinone methide precursors.

5-Substituted Compounds

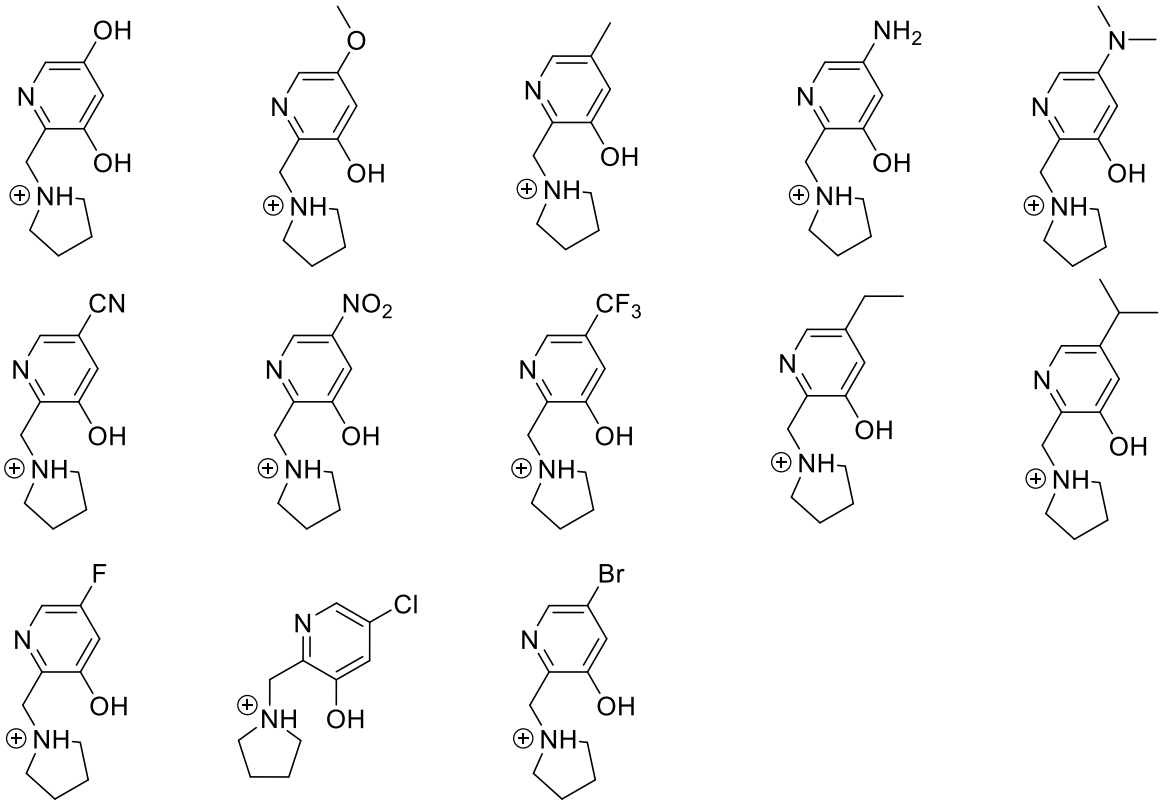

Figure 2.3: Library of quinone methide precursors

6-Substituted Compounds

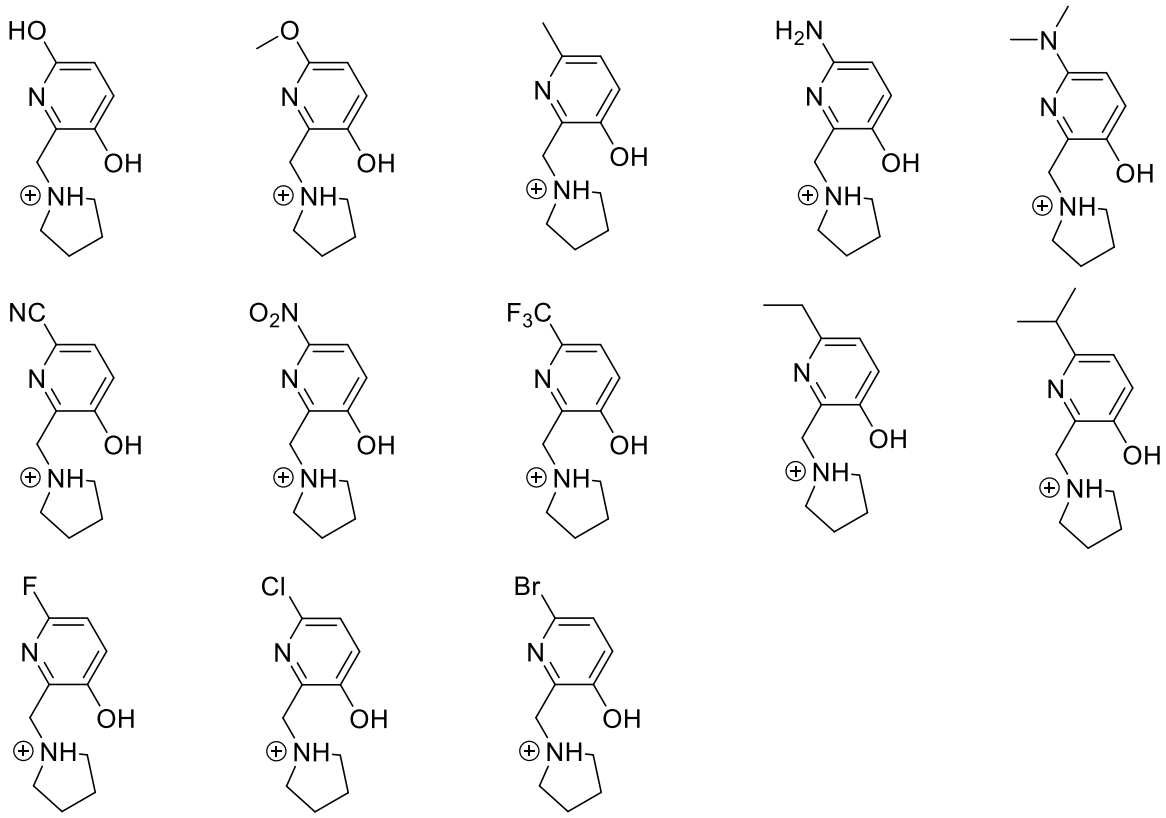

Figure 2.4: Library of quinone methide precursors

2.2 Preparation of structures for Docking

To prepare these molecules for docking in the crystal structure of aged AChE each molecule was manually built in GaussView (Version 4.1.2) [1]. The B3LYP/6-311+G** level of theory was used for all calculations. Then they were all structurally optimized with Gaussian 09 with a Polarizable Continuum Model (PCM) of solvation in water [2], [3]. These optimizations yield the lowest energy conformation of the molecule which was then subjected to vibrational frequency analysis to confirm that the geometry was a minimum on the potential energy surface. To complete their preparation Merz-Kollman charge calculations were performed to each compound's lowest energy conformation to build an electrostatic potential surface [4].

These final geometries are reasonable approximations of their physical counterparts as the B3LYP density functional theory (DFT) method with the 6-311G** basis set has been shown to produce structural geometries very similar to those found via x-ray crystallography [5], [6].

2.3 Docking

Molecular Docking (MD) is a computational technique that is used to predict the predominant binding modes of a ligand within a protein active site by modeling the electrostatic interactions of the two. The ligand can move, flex, and rotate within the active site of the protein, which is held static. The simulation will move the ligand to increase favorable interactions in the active site and decrease steric clashes and unfavorable charge interactions. The resulting poses of the ligand within the active site can be used to predict ligand affinity for the active site.

The prepared QMPs were docked in the active sites of 13 different poses of an artificially aged human AChE structure (PDB: 1B41). The structure of 1B41 was altered by the removal of the bound fasciculin peptide, cofactors, waters, and the addition of a phosphonate to the Ser_{203} residue. These frames were used because the shape of the active site of AChE changes slightly as the enzyme structure naturally oscillates slightly on a nanosecond timescale [7]. These 13 frames are static representations produced from a 5 nanosecond molecular dynamics simulation of AChE with a standard QMP in the active site so that the effects of induced fit could be analyzed with static enzyme structures, which reduces simulation complexity and lowers the required computational power.

The QMPs were docked using Autodock4[8] in a 50x50x50 Å grid box positioned to contain the active site and part of the gorge leading from the surface of the enzyme to the active site. Then for every QMP 200 poses of the ligand in the active site for each of the receptor frames were saved, providing 2600 total poses per QMP across all 13 frames.

After finishing these docking simulations, the compounds' abilities to bind in the active site were scored by using the distance between the benzylic carbon (Figure 2.5) of the ligand and the oxygen of the phosphonate on the Ser_{203} residue. The bond necessary for the realkylation event is formed between these two atoms, and we hypothesize that the more poses where the distance between the two atoms is under 5 Å the higher the probability of the desired reaction occurring.

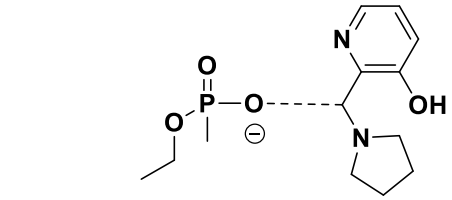

Phosphonylated Serine QMP

Figure 2.5: The dotted line from the phosphonate oxygen to the benzylic carbon of the QMP is the distance used to score the putative realkylating activity of a ligand.

2.4 Docking results

After scoring the ligands using the phosphonate- benzylic carbon distances some interesting trends can be seen. The 4-substituted molecules scored better and have smaller distances overall than the 5-substituted molecules which in turn outperform the 6-substituted molecules.

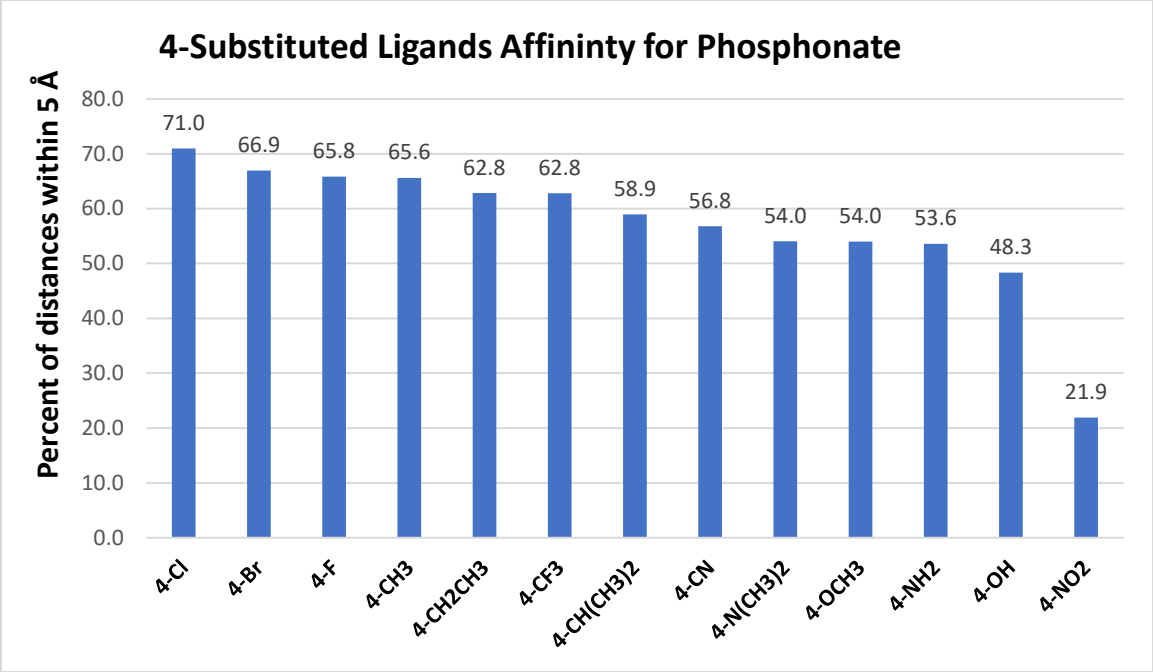

Figure 2.6: Docking percentage affinity of ligands with substitutions at their 4 position for the active site of AChE. The score depicted above each bar is the percent of output poses where the benzylic carbon of the ligand is within 5 Å of the phosphonate oxygen that points into the active site which is always the closest.

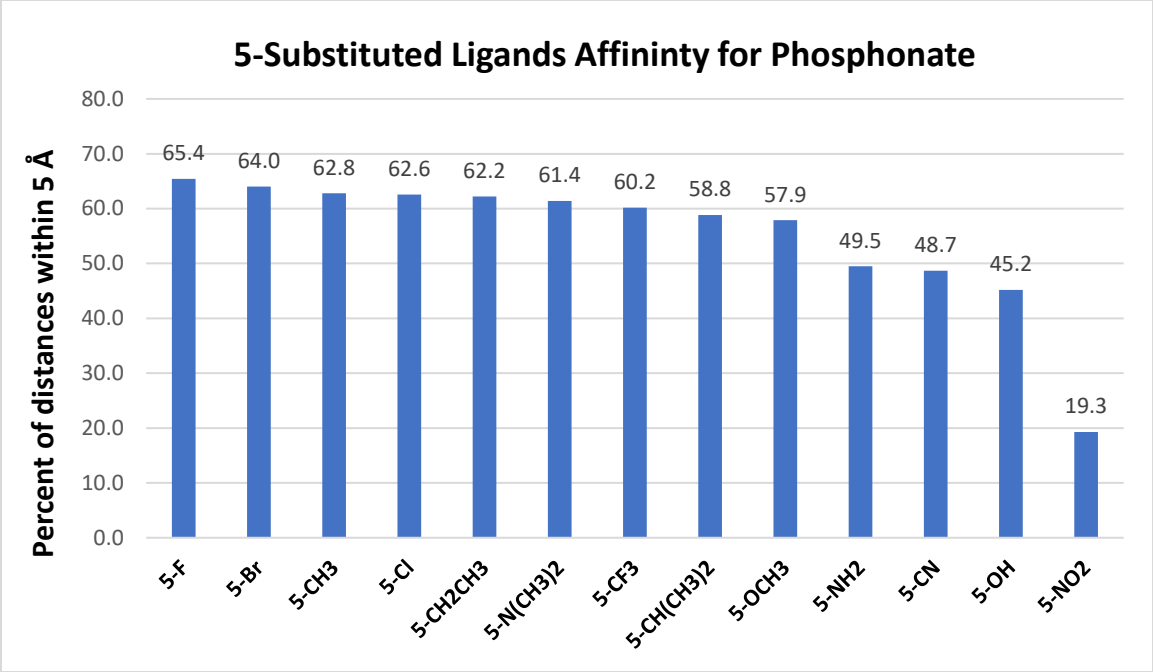

Figure 2.7: Docking percentage affinity of ligands with substitutions at their 5 position for the active site of AChE. The score depicted above each bar is the percent of output poses where the benzylic carbon of the ligand is within 5 Å of the closest phosphonate oxygen.

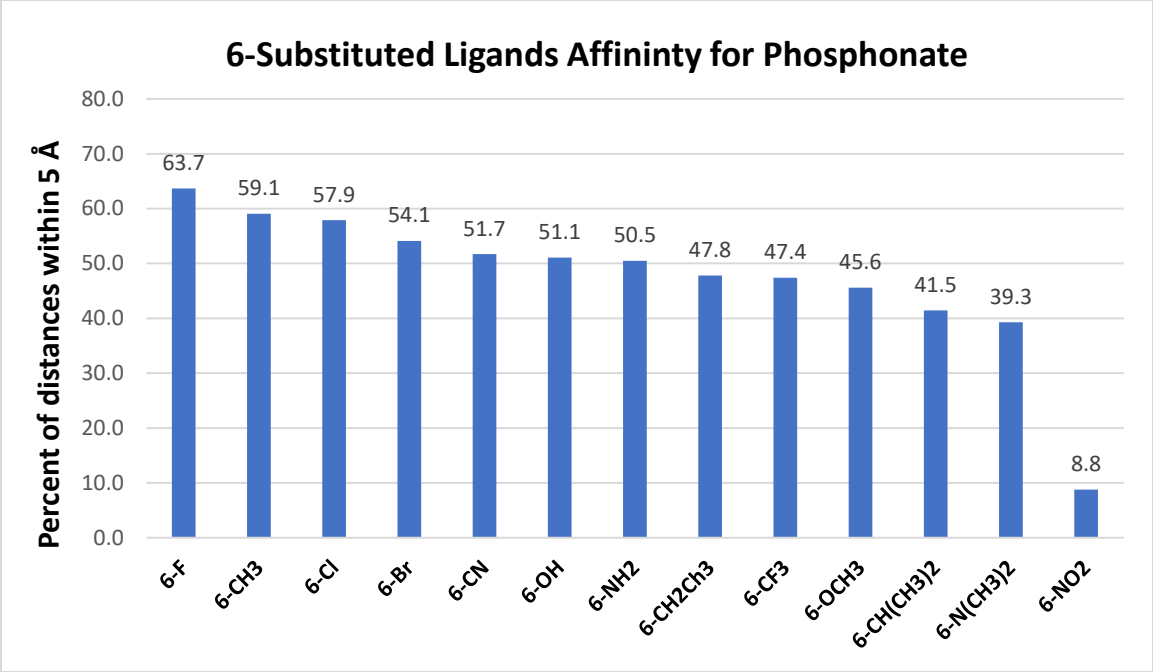

Figure 2.8: Docking percentage affinity of ligands with substitutions at their 6 position for the active site of AChE. The score depicted above each bar is the percent of output poses where the benzylic carbon of the ligand is within 5 Å of the closest phosphonate oxygen.

Qualitative analysis of the docking output which shows ligands in different conformations indicates that this trend of decreasing affinity is due to two effects, first the 5 and 6 position substitutions direct the ligands to spend more time interacting with residues in the bottleneck. (Figure 2.9) This prevents the ligand from getting as close to the aged Ser_{203} residue as the 4 substituted frameworks.

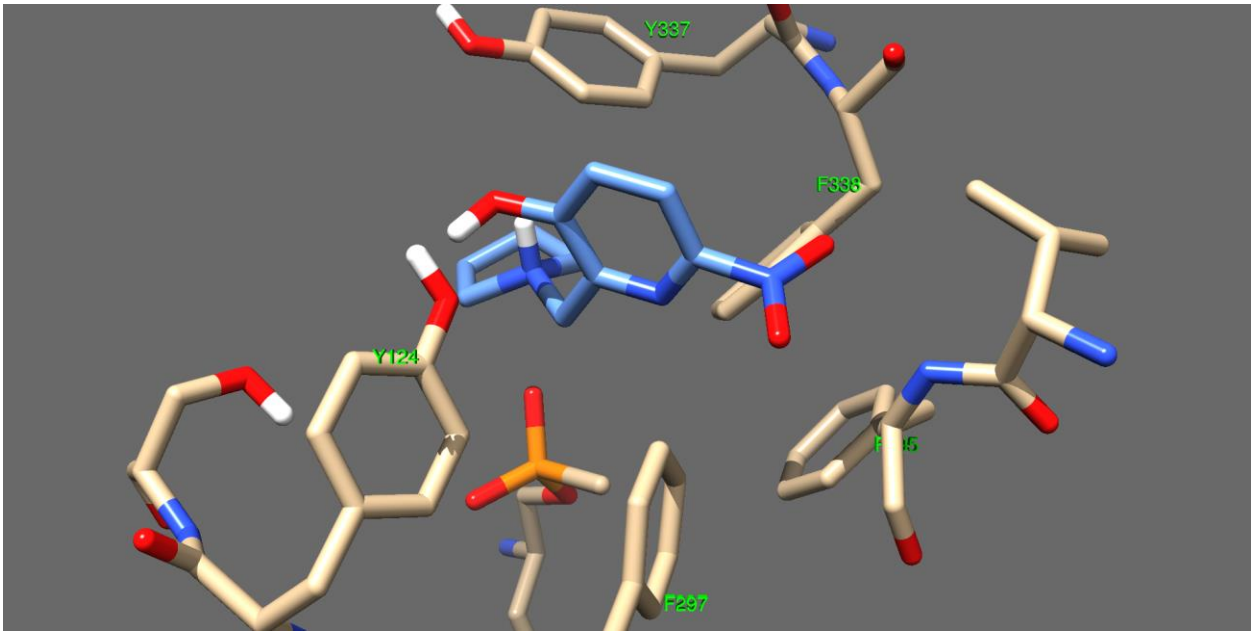

Figure 2.9: 6-NO_3-corriganine is interacting with the residues Phe_{295}, Phe_{297}, Phe_{338}, and hydrogen bonding with Tyr_{124}. These residues are part of the bottleneck section of the binding pocket that is located between the opening and the catalytic triad. The steric effect of the 5 and 6 position substituents direct them to the bottleneck area.

Ligand	Score
R=4-Cl	71.0
R=4-Br	66.9
R=4-F	65.8
R=4-CH_3	65.6
R=5-F	65.4
R=5-Br	64.0
R=6-F	63.7
R=4-CH_2CH_3	62.8
R=4-CF_3	62.8
R=5-CH_3	62.8
R=5-Cl	62.6
R=5-CH_2CH_3	62.2
R=5- $N(CH_3)_2$	61.4
R=5-CF_3	60.2
R=6-CH_3	59.1
R=4-$CH(CH_3)_2$	58.9
R=5- $CH(CH_3)_2$	58.8
R=5-OCH_3	57.9
R=6-Cl	57.9
R=4-CN	56.8
R=6-Br	54.1
R=4-$N(CH_3)_2$	54.0
R=4-OCH_3	54.0
R=4-NH_2	53.6
R=6-CN	51.7
R=6-OH	51.1
R=6-NH_2	50.5
R=5-NH_2	49.5
R=5-CN	48.7
R=4-OH	48.3
R=6-CH_2CH_3	47.8
R=6-CF_3	47.4
R=6-OCH_3	45.6
R=5-OH	45.2
R=6-$CH(CH_3)_2$	41.5
R=6-$N(CH_3)_2$	39.3
R=4-NO_2	21.9
R=5-NO_2	19.3
R=6-NO_2	8.8

Table 2.1: ligands ranked by percent of the 2600 docking poses with distances of 5 Å or lower to the phosphonate oxygen.

The expected distribution of these high performing ligands can be seen. The majority of measured distances are within the 3-4 Å distance which is optimal, and the number of poses found in outer regions of the binding pocket are minimal. (Figure 2.8) This is the localization that would be desirable for a good realkylator to exhibit *in vitro* as time spent near the phosphylated serine should increase the likelihood of a reaction.

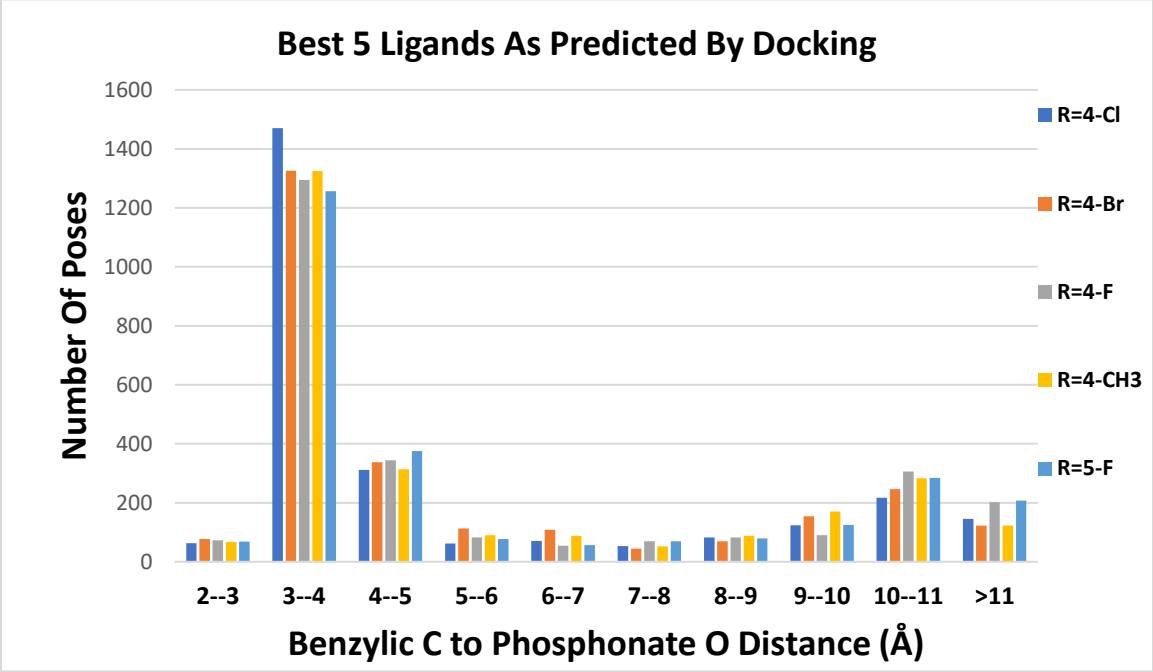

Figure 2.10: Here the 2600 total poses for each ligand have been sorted by their distance from the phosphonate. Only the top five compounds are pictured.

Molecular Dynamics

Molecular dynamics (MD) is a computational technique that models ligand interactions within a fluid and dynamic model over a set period of time. Allowing both ligand and enzyme to move with constraints. Allowing this additional motion creates a better approximation than molecular docking of the evolution of the system over time. For this set of MD calculations, water was designated as the solvent, and the three most energetically favorable poses from molecular docking are used as starting geometry for the system. All 13 frames of the prepared AChE were used as MD starting geometries

resulting in a total 39 MD simulations for each ligand. This system has some energy outliers, so a steepest descent minimization is run for 500 steps followed by 500 steps of a conjugate gradient minimization calculation to push the system to a more accurate energy level. The system is put through another 1000 steps of steepest descent minimization and 1500 steps of conjugate gradient minimization before beginning the actual MD simulation with a timescale of 1 nanosecond.

As the ligand moves its time spent in three designated sections of AChE; the gorge mouth, the bottleneck, and the active site, are used to determine if it would be an effective therapeutic for use in regenerating the enzyme. These sections of the enzyme are labeled based on their distance from the phosphylated Ser_{203} residue, which were empirically derived from initial simulations.

Binding Pocket Location	Angstroms from Phosphonate Oxygen
Active Site	0-5 Å
Active site to Bottleneck	5-7 Å
Bottleneck	7-9.5 Å
Gorge Mouth	15 Å+

Table 2.2: Distances between benzylic carbon and phosphonate oxygen that form scoring criteria for MD simulation

The results of molecular dynamics calculations were compiled to yield quantitative data on the ligands' binding preferences as a percent of poses with distances below 5 Å.

2.6 Molecular Dynamics Results

Tables of results for each ligand were produced by measuring the distance from the benzylic carbon of the ligand to the oxygen of the phosphylated Ser_{203}. The MD simulation produces 500

snapshot frames over 1 nanosecond for each cluster. The typical total of still frames output from MD was 19500 frames gathered from each of the 3 clusters for each of the 13 frames. Each frame was sorted into the bins based on their ligand to Ser_{203} distances. The number of frames in each bin was divided by the total frames for the ligand and shown as a percent of frames in a specific bin.

Substituent	% Active Site	% Between AS and BN	% Bottleneck	% Between BN and GM	% Gorge Mouth
4-OH	35.22	19.16	19.01	3.08	22.46
4-OCH_3	54.01	20.1	4.26	1.19	20.44
4-CH_4	33.81	23.91	27.23	3.44	11.59
4-NH_2	47.23	23.41	9.69	2.36	17.2
4-$N(CH_3)_2$	44.38	22.21	19.11	5.73	8.57
4-CN	50.68	11.83	13.84	4.91	17.33
4-NO_2	24.95	16.87	22.99	2.48	30.68
4-CF_3	44.27	13.83	13.28	3.58	24.96
4-CH_2CH_3	68.29	8.99	9.54	2.67	10.51
4-$CH(CH_3)_2$	51.48	14.9	3.78	1.77	27.97
4-F	54.78	12.33	9.75	7.16	15.98
4-Cl	63.85	26.28	0.95	1.35	7.57
4-Br	48.94	28.76	9.27	2.28	10.32

Table 2.3: 4-substituted ligand populations as percent of distances measured to closest aged phosphonate oxygen. (AS)=active site (BN)= bottleneck, (GM)= gorge mouth.

Substituent	% Active Site	% Between AS and BN	% Bottleneck	% Between BN and GM	% Gorge Mouth
R=5-OH	76.7	13.3	6.0	0.4	3.6
R=5-OCH_3	51.0	24.9	7.1	2.8	13.9
R=5-CH_4	60.3	17.2	2.4	1.4	18.8
R=5-NH_2	79.3	12.6	3.5	2.4	2.3
R= $N(CH_3)_2$	41.3	31.1	10.2	4.6	12.9
R=5-CN	38.1	32.9	3.3	2.2	21.7
R=5- NO_2	22.5	30.9	16.0	2.3	25.5
R=5- CF_3	39.8	20.9	11.5	3.7	23.1
R=5- CH_2CH_3	47.1	30.0	6.5	0.6	15.8
R=5- $CH(CH_3)_2$	46.8	18.0	8.0	0.4	25.6
R=5-F	62.2	23.7	1.2	0.2	12.7
R=5-Cl	54.4	27.3	1.1	1.9	15.0
R=5-Br	52.0	23.8	3.6	2.2	18.4

Table 2.4: 5-substituted ligand populations as percent of distances measured to aged phosphonate oxygen. (AS)=active site (BN)= bottleneck, (GM)= gorge mouth.

Compound Name	% Active Site	% Between AS and BN	% Bottleneck	% Between BN and GM	% Gorge Mouth
R=6-OH	47.3	28.6	9.7	0.3	8.9
R=6-OCH_3	53.2	8.7	8.2	3.7	21.1
R=6-CH_3	51.8	13.2	14.9	1.3	13.7
R=6-NH_2	43.3	20.5	22.1	1.8	5.8
R=6-$N(CH_3)_2$	22.2	30.4	14.7	3.3	21.8
R=6-CN	29.0	31.1	10.1	0.9	13.2
R=6-NO_2	30.4	20.9	10.8	4.1	22.5
R=6-CF_3	44.2	16.7	6.7	2.2	17.7
R=6-CH_2CH_3	45.0	9.6	12.7	1.7	17.9
R=6-$CH(CH_3)_2$	45.7	11.1	11.3	1.5	20.2
R=6-F	39.2	33.9	8.7	0.7	11.4
R=6-Cl	32.9	37.3	11.0	1.1	11.2
R=6-Br	28.7	37.5	13.7	2.1	11.6

Table 2.5: 6-substituted ligand populations as percent of distances measured to aged phosphonate oxygen. (AS)=active site (BN)= bottleneck, (GM)= gorge mouth.

Interestingly the top preforming ligands in docking were not conserved in MD, the 5-halogen substituted corriganine were best in docking but in MD the 5-OH, 5-CH_3, and 5-NH_3 were the best preforming ligands. These ligands spend a significant amount of time hydrogen bonding with the methyl-phosphonate and Glu_{202}. (Figures 2.11, 2.12, 2.13, 2.14) They also show frequent Trp_{86} pi-pi interaction with both rings of the ligand. The reason for this discrepancy between some docking and MD results are likely because MD is a more accurate predictor of enzyme-ligand interaction with its fluid protein structure which can move in response to the presence of the ligand, where docking uses only static poses of the protein.

Ligand	Score
R=5-NH_2	79.3
R=5-OH	76.7
R=4-CH_2CH_3	68.3
R=4-Cl	63.9
R=5-F	62.2
R=5-CH_3	60.3
R=4-F	54.8
R=5-Cl	54.4
R=4-OCH_3	54.0
R=6-OCH_3	53.2
R=5-Br	52.0
R=6-CH_3	51.8
R=4-$CH(CH_3)_2$	51.5
R=5-OCH_3	51.0
R=4-CN	50.7
R=4-Br	48.9
R=6-OH	47.3
R=4-NH_2	47.2
R=5-CH_2CH_3	47.1
R=5-$CH(CH_3)_2$	46.8
R=6-$CH(CH_3)_2$	45.7
R=6-CH_2CH_3	45.0
R=4- $N(CH_3)_2$	44.4
R=4-CF_3	44.3
R=6-CF_3	44.2
R=6-NH_2	43.3
R=5-$N(CH_3)_2$	41.3
R=5-CF_3	39.8
R=6-F	39.2
R=5-CN	38.1
R=4-OH	35.2
R=4-CH_3	33.8
R=6-Cl	32.9
R=6-NO_2	30.4
R=6-CN	29.0
R=6-Br	28.7
R=4-NO_2	25.0
R=5-NO_2	22.5
R=6-$N(CH_3)_2$	22.2

Table 2.6: Molecular Dynamics ligand scores (% of poses within 5 Å).

The trend of low active site affinity among 6-position substitutions seen in docking was maintained in MD. The preference of these ligands to interact with the bottleneck predicted by docking continued to be a factor, which increases the likelihood that these 6-substituted ligands will perform poorly *in vitro*.

Substituent	Average Score	Electrophilic aromatic directing Properties
NH_2	57	Strong electron donating
CH_2CH_3	53	Weak electron donating
OH	53	Strong electon donating
OCH_3	53	Strong electron donating
F	52	Weak electron withdrawing
Cl	50	Weak electron withdrawing
CH_3	49	Weak electron donating
$CH(CH_3)_2$	48	Weak electron donating
Br	43	Weak electron withdrawing
CF_3	43	Strong electron withdrawing
CN	39	Strong electron withdrawing
$N(CH_3)_2$	36	Strong electron donating
NO2	26	Strong electron withdrawing

Table 2.7: Here the scores (% of distances <5 Å) for each substituent type from the MD simulation were averaged from the 4, 5, and 6 position tests and the substituents were then ranked where the top NH_2 group is the best at directing ligands to the active site and the bottom NO_2 is the worst. Each substituent electrophilic aromatic directing properties are also displayed.

The three worst preforming substituent groups, NO_2, $N(CH_3)_2$, and the nitrile groups were poor in docking and MD, because their bulky substituents kept them interacting with residues in the gorge mouth and bottleneck (Figure 2.9), as evidenced by their low percent of distances near the phosphonate. (Tables 2.6, 2.7) In terms of groups that modify the electron density of the pyridine ring, the electron donating groups (NH_2, CH_2CH_3, OH, OCH_3) all performed well while three of the worst groups were exclusively strong electron withdrawing groups, except for $N(CH_3)_2$, indicating that strong electron donating groups are better at directing ligands into the active site.

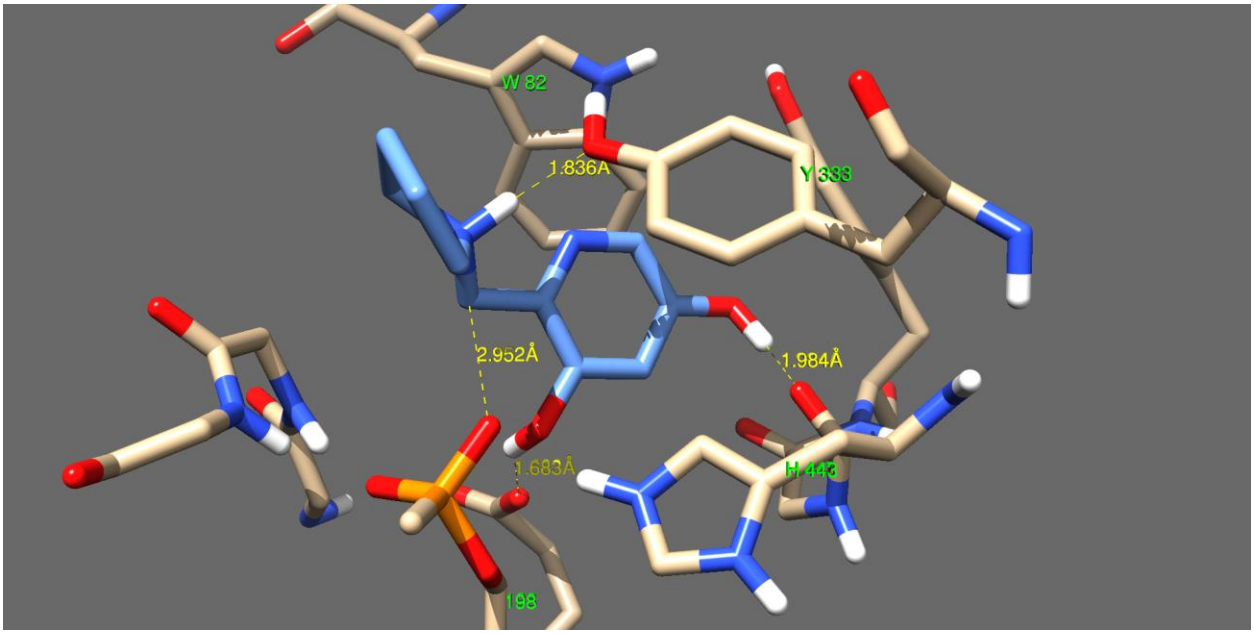

Figure 2.11: MD output pose for 5-OH-corriganine in the active site of AChE.

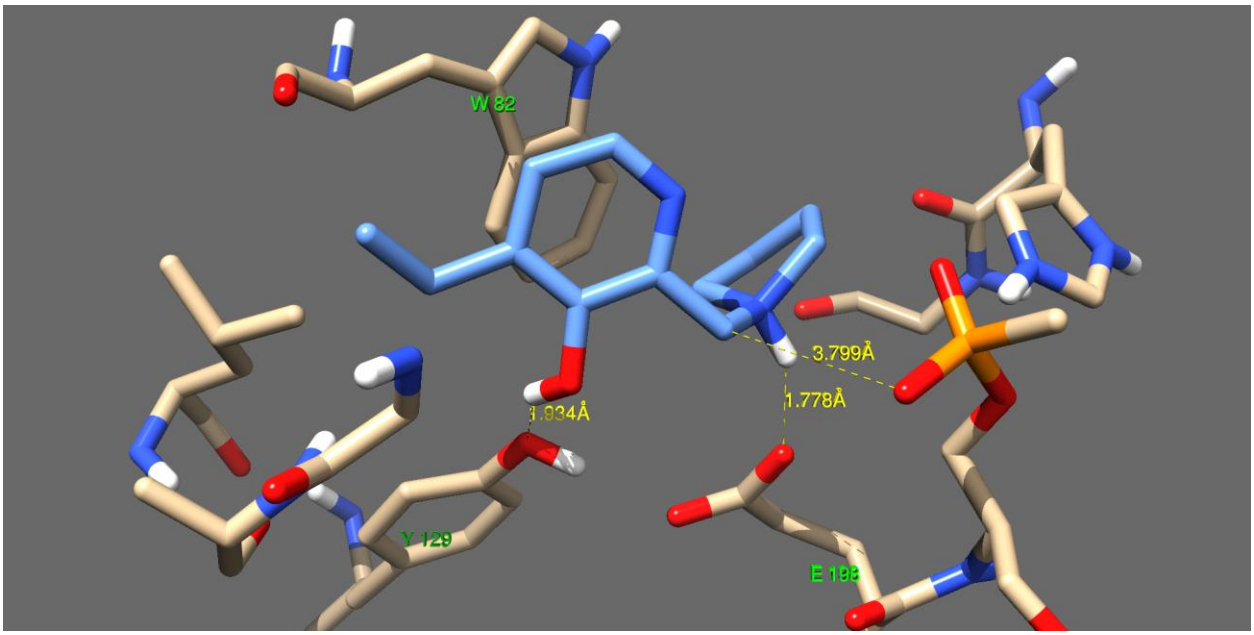

Figure 2.12: MD output pose for 4-CH_2CH_3-corriganine (blue).

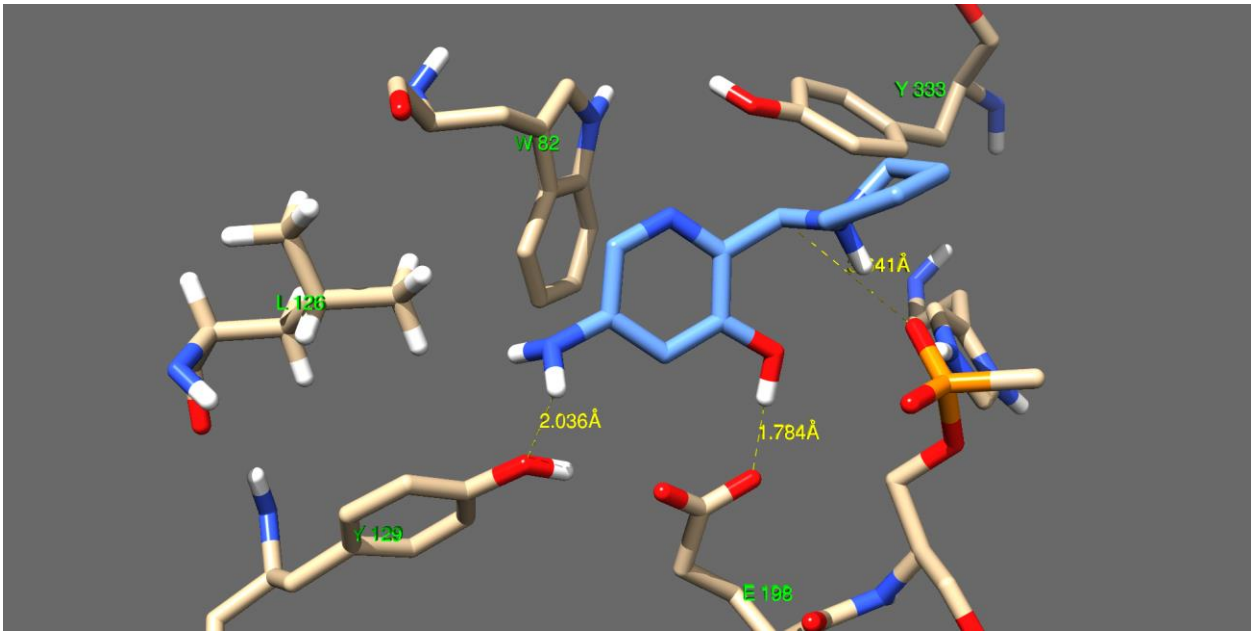

Figure 2.13: MD output pose for 5-NH_2-corriganine (blue).

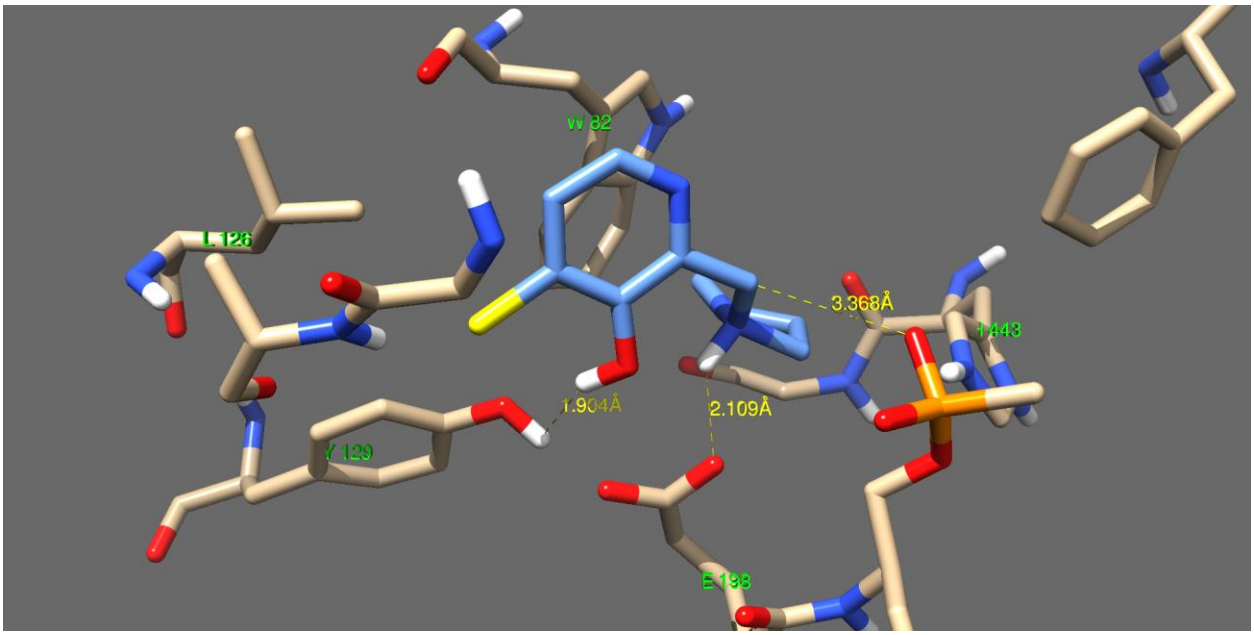

Figure 2.14: MD output pose for 4-Cl-corriganine (blue).

The best performing ligands (Figures 2.11, 2.12, 2.13, 2.14) all occupy a similar location in the active site, above the Glu_{202} and to the left of the phosphonate (looking from the phosphonate outward). This is likely because this is the location with the densest cluster of hydrogen bond donors and accepting residues, namely Ser_{203}, Glu_{202}, and Tyr_{133}.

The 3 position hydrogen bonds with the methyl-phosphate, while the 5-OH forms a hydrogen bond with the carbonyl oxygen of the His_{452} residue. (Figure 2.11) The pyrrolidine hydrogen bonds with the Tyr_{341} residue. The pyrrolidine hydrogen bonds with Glu_{202}, while the hydroxyl forms a hydrogen bond with Tyr_{137}. Trp_{86} pi stacking occurs in almost all frames. The ethyl group is within Van Der Waals interaction distance of the Lys_{134} residue. (Figure 2.12) The amino group hydrogen bonds with Tyr_{137} while the pyrrolidine hydrogen bonds with the phosphate and the hydroxyl forms a hydrogen bond with Glu_{202}. (Figure 2.13) The 3-OH group hydrogen bonds with Tyr_{137} while the pyrrolidine nitrogen hydrogen bonds with the Glu_{202} residue. (Figure 2.14)

Across all frames with 4-Cl-corriganine (Figure 2.14) the chlorine atom does not exhibit any discrete interactions, however, its position may sterically discourage other positions with less favorable distances to the phosphonate. Additionally, the weak electron-withdrawing properties of halide substitution could be lessening the effect of the Trp_{86} pi-pi interactions which would allow the ligand to pull away from that residue toward the phosphonate.

2.7 References

[1] GaussView, Version 4.1.2, Dennington, Roy; Keith, Todd; Millam, John. Semichem Inc., Shawnee Mission, KS, 2009.

[2] Gaussian 09, Revision D.01, Frisch, M. J.; Trucks, G. W.; Schlegel, H. B.; Scuseria, G. E.; Robb, M.A.; Cheeseman, J. R.; Scalmani, G.; Barone, V.; Mennucci, B.; Petersson, G. A.; Nakatsuji, H.; Caricato, M.; Li, X.; Hratchian, H. P.; Izmaylov, A. F.; Bloino, J.; Zheng, G.; Sonnenberg, J. L.; Hada, M.; Ehara, M.; Toyota, K.; Fukuda, R.; Hasegawa, J.; Ishida, M.; Nakajima, T.; Honda, Y.; Kitao, O.; Nakai, H.; Vreven, T.; Montgomery, J. A., Jr.; Peralta, J. E.; Ogliaro, F.; Bearpark, M.; Heyd, J. J.; Brothers, E.; Kudin, K. N.; Staroverov, V. N.; Kobayashi, R.; Normand, J.; Raghavachari, K.; Rendell, A.; Burant, J. C.; Iyengar, S. S.; Tomasi, J.; Cossi, M.; Rega, N.; Millam, N. J.; Klene, M.; Knox, J. E.; Cross, J. B.; Bakken, V.; Adamo, C.; Jaramillo, J.; Gomperts, R.; Stratmann, R. E.; Yazyev, O.; Austin, A. J.; Cammi, R.; Pomelli, C.; Ochterski, J. W.; Martin, R. L.; Morokuma, K.; Zakrzewski, V. G.; Voth, G. A.; Salvador, P.; Dannenberg, J. J.; Dapprich, S.; Daniels, A. D.; Farkas, Ö.; Foresman, J. B.; Ortiz, J. V.; Cioslowski, J.; Fox, D. J. Gaussian, Inc., Wallingford CT, 2009.

[3] Mennucci, B. (2012), Polarizable continuum model. WIREs Comput Mol Sci, 2: 386–404. doi: 10.1002/wcms.1086

[4] Pettersen, E. F.; Goddard, T. D.; Huang, C. C.; Couch, G. S.; Greenblatt, D. M.; Meng, E. C.; Ferrin, T. E. J. Comput. Chem. 2004, *25*, 1605-1612.

[5]. Beck, J. M., Ph.D. thesis, The Ohio State University, 2011

[6] A.D. Becke, J.Chem.Phys. 98 (1993) 5648-5652

[7] *Acetylcholinesterase: enzyme structure, reaction dynamics, and virtual transition states Daniel M. Quinn.* Chemical Reviews *1987* 87 *(5), 955-979. DOI: 10.1021/cr00081a005*

[8] Morris, G. M., Huey, R., Lindstrom, W., Sanner, M. F., Belew, R. K., Goodsell, D. S. and Olson, A. J. (2009) Autodock4 and AutoDockTools4: automated docking with selective receptor flexiblity. J. Computational Chemistry 2009, 16: 2785-91.

[9] P.J. Stephens, F.J. Devlin, C.F. Chabalowski, M.J Frisch, J.Phys.Chem. 98 (1994) 11623-11627

[10]. Blanton, Travis. Thesis, The Ohio State University, 2015

[11] Case, D. A.; Darden, T. A.; Cheatham, T. E., III; Simmerling, C. L.; Wang, J.; Duke, R. E.; Luo, R.; Crowley, M.; Walker, R. C.; Zhang, W.; Merz, K. M.; Wang, B.; Hayik, S.; Roitberg, A.; Seabra, G.; Kolossváry, I.; Wong, K. F.; Paesani, F.; Vanicek, J.; Wu, X.; Brozell, S. R.; Steinbrecher, T.; Gohlke, H.; Yang, L.; Tan, C.; Mongan, J.; Hornak, V.; Cui, G.; Mathews, D. H.; Seetin, M.G.; Sagui, C.; Babin, V.; Kollman, P. A. AMBER 11, University of California, San Francisco, 2008.

[12] Molecular graphics and analyses were performed with the UCSF Chimera package. Chimera is developed by the Resource for Biocomputing, Visualization, and Informatics at the University of California, San Francisco (supported by NIGMS P41-GM103311).

[13] Persistence of Vision Pty. Ltd. (2004). Persistence of Vision (TM) Raytracer. Persistence of Vision Pty. Ltd., Williamstown, Victoria, Australia. http://www.povray.org/

[14] Humphrey, W., Dalke, A. and Schulten, K., "VMD - Visual Molecular Dynamics", J. Molec. Graphics, 1996, vol. 14, pp. 33-38.

3 Tomographic Docking

3.1 Introduction

Tomodock is a program provided free by researchers at the University of Warwick in the UK that utilizes sequential Autodock Vina docking simulations to analyze interactions between protein residues and ligands along the length of deep enzyme binding pockets [1].

Tomodock allows the user to specify two or more points marking the opening and the bottom of the binding pocket. Several grid boxes whose dimensions and quantity are specified by the user are spaced evenly between the two endpoints and run sequentially. At each depth the chosen ligand can interact with only the residues that intersect the gridbox and the lowest energy pose is found and saved. This will yield a series of poses from the mouth of the pocket to the bottom showing a lowest energy path of diffusion.

Tomodock was used to reveal interactions between Corriganine and the residues along the binding pocket of AChE. The interactions that Corriganine is seen to favor as it moves down the active site can be compared to the interactions that a non- resurrecting QMP favors during a simulation to isolate those interactions that serve to aid QMP diffusion to the methyl-phosphonate bound serine, and those that that inhibit movement down the pocket. Once known we can then use a combination of further *in silico* and *in vitro* techniques to design QMPs intelligently, so that they will better navigate the length of the binding pocket and realkylate the phosphonate with greater speed and reliability.

3.2 Tomodock Analysis Methods

For our simulations we used six gridboxes to cover the entire topography of the binding pocket. Boxes had initial coordinates x-60 y-37.9 z-42.7 and final coordinates x-48.8 y-37.9 z-42.7 (Figure 3.1) and box dimensions were 16 angstroms square and 6 angstroms tall. The simulation was run with three different versions of Corriganine, a protonated amine, a zwitterionic form, and a neutral form. The simulation was run in thirteen different frames of human acetylcholinesterase (PDB 1B41). These frames

were collected from an MD simulation of the enzyme to represent the dynamic motion it would exhibit in solution. Some of the outputs from these frames were unsuitable because the bottleneck was occluded by residues, and these were discarded.

3.3 Analysis and Results

The positive, neutral and zwitterionic states exhibited similar patterns of interaction as they moved down the active site. (Figures 3.3, 3.4, and 3.5) The Zwitterionic form has a slightly lower overall binding energy, likely because of the greater amount of hydrogen bonds it can form in the active site.

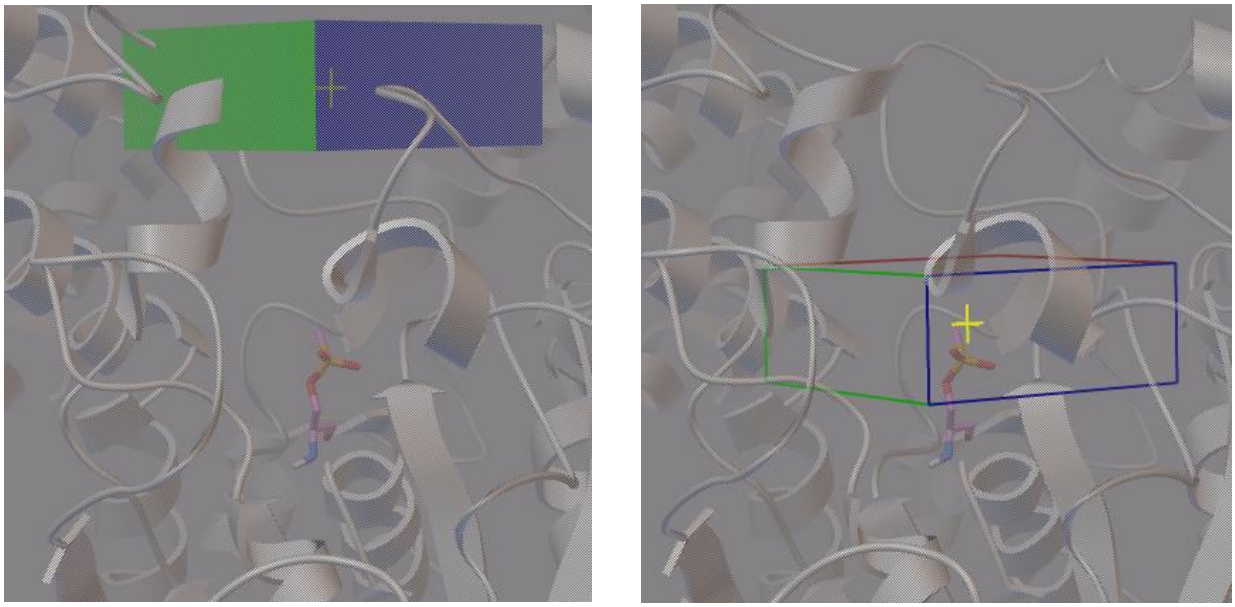

Figure 3.1: Starting Position of Tomodock gridbox (Left) and the ending point (Right).

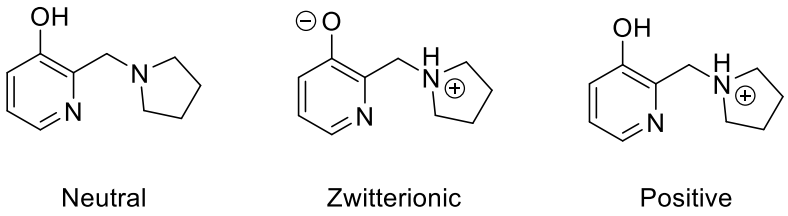

Figure 3.2: Pictured are the three charge states of corriganine that were tested in Tomodock.

As the positively charged corriganine moves down the gorge into the active site it avoids the oxyanion hole (blue) except for a transient hydrogen bond with Ser_{125}. (Figure 3.3) The positive corriganine also has heavily conserved pi-pi interaction with the Trp_{86} residue in the cation binding region (orange).

The neutral Corriganine ligand moves down the gorge into the active site while avoiding the oxyanion hole (blue) and has heavily conserved pi stacking with the Trp_{86} residue in the cation binding region (orange). (Figure 3.4) The ligand forms a hydrogen bond with Tyr_{124}. Like the positive ion orientations but with no Ser_{125} interaction. The zwitterion has a similar path to the positive ion however it avoids interaction with Ser_{125}.

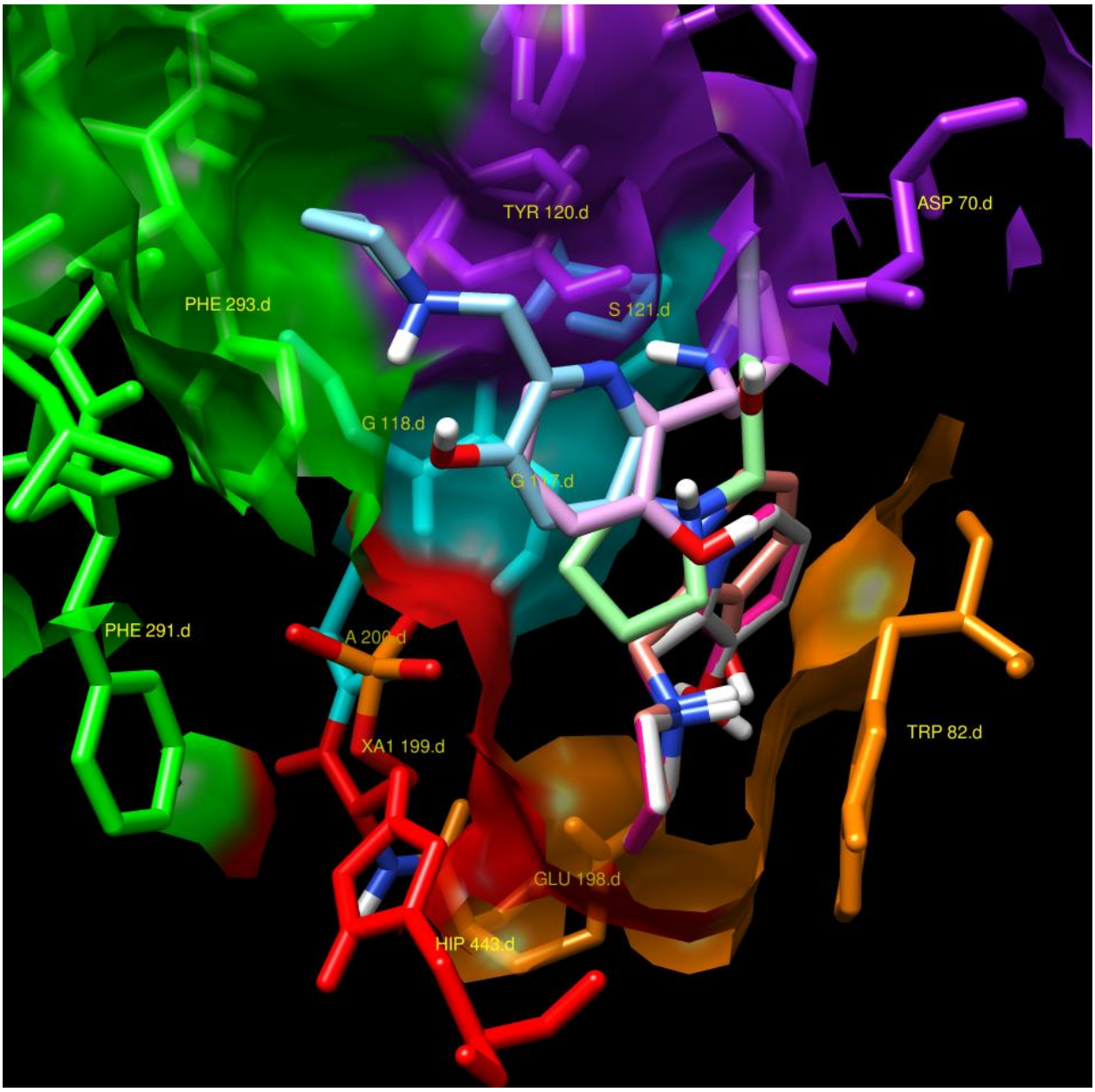

Figure 3.3: Results from each of the Tomodock simulations with positively charged corriganine. The catalytic triad surface is red, the acyl loop is depicted here in green, and the purple area is the omega loop/ active site.

Figure 3.4: Results from each of the Tomodock simulations with neutral charged corriganine. The catalytic triad surface is red, the acyl loop is depicted here in green, and the purple area is the omega loop/ active site.

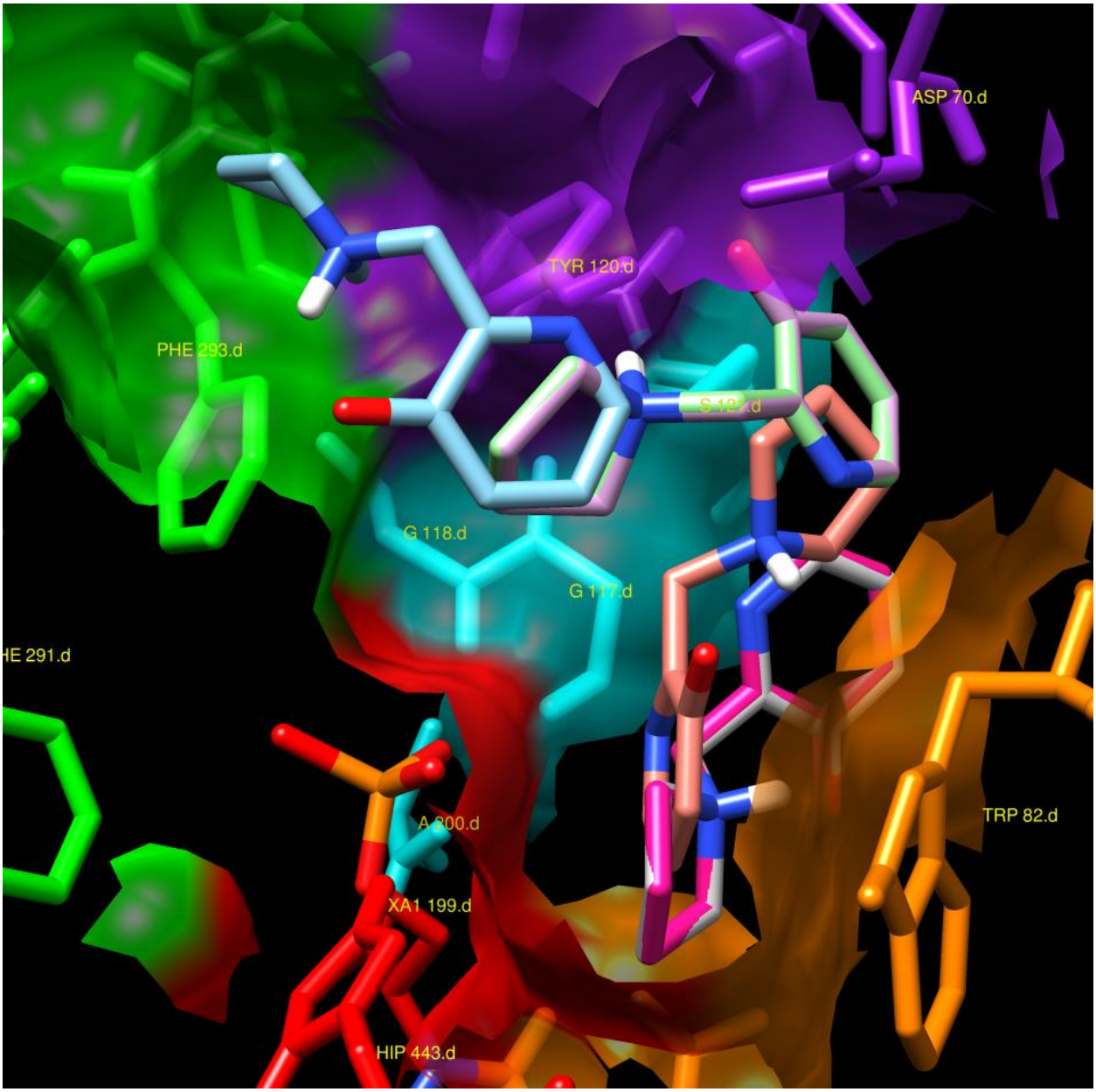

Figure 3.5: Results from each of the Tomodock simulations with zwitterion form of corriganine. The catalytic triad surface is red, the acyl loop is depicted here in green, and the purple area is the omega loop/ active site.

The binding energies of corriganine in these charge states differs, with the zwitterion having the lowest, followed by the positively charged corriganine. (Figure 3.6) This predicts that ligands with better or more hydrogen bonding groups or ionic interactions will have more favorable interactions within the binding pocket, and that future ligand research should utilize this knowledge.

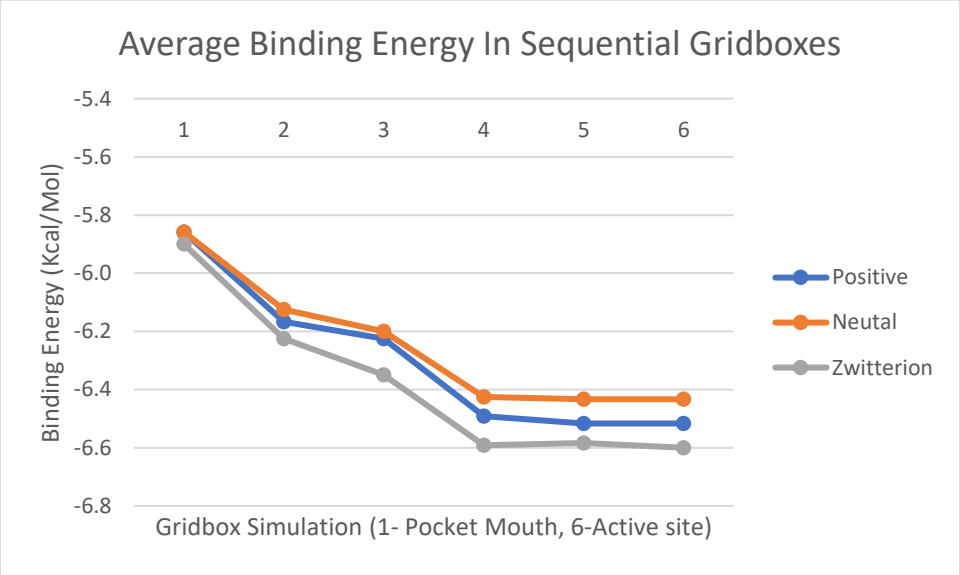

Figure 3.6: Autodock Vina binding energies outputs for each of the charge states of corriganine as it diffuses down the active site of human AChE. Each numbered gridbox is a new Autodock Vina simulation at a lower xyz coordinate between the entrance of the binding pocket to the catalytic triad.

The binding energies of the three charged states indicates that the zwitterion form had the lowest energy states over the course of the simulated diffusion of the ligand to the active site.

3.9 References

[1] Tomographic docking suggests the mechanism of auxin receptor TIR1 selectivity Veselina V. Uzunova, Mussa Quareshy, Charo I. del Genio, Richard M. Napier Open Biol. 2016 6 160139; DOI: 10.1098/rsob.160139. Published 19 October 2016

[2] O. Trott, A. J. Olson, AutoDock Vina: improving the speed and accuracy of docking with a new scoring function, efficient optimization and multithreading, Journal of Computational Chemistry 31 (2010) 455-461

4 Conclusions and Future Work

4.1 Conclusion

The ligands that scored the best in MD simulation results are the best candidates for realkylating methyl-phosphonate aged AChE. The trend among the best scoring ligands from MD was for additional hydrogen bonding groups (5-NH_2 and 5-OH) or a 4-CH_2CH_3 group. The rest of the top ten compounds had halide or methyl substitutions however their score was far below the top three compounds.

The 5-OH and 5-NH_3 substituted ligands (scores 70.3 and 61.3 respectively) show a greater affinity for Glu_{202} than other residues in the active site. This helps position the ligand more closely to the phosphonate and minimize the distance from the benzylic carbon to the phosphonate, increasing the probability of the desired reaction.

The 4-CH_2CH_3 substitution was found most often interacting with the two groups of hydrophobic residues in the active site (Phe_{338}, Try_{341}, Trp_{86}, and leu_{130}) these interactions pull the pyridine ring away from the Trp_{86} residue and toward the phosphonate. pi-pi interactions between the heterocycles of the Trp_{86} residue and the ligand pyridine pull the ligand away from the phosphonate and it appears that the 4-CH_2CH_3 substituent counteracts this. (Table 2.7)

Among the compounds with the lowest affinity for the active site, large sterically hindering substituents like the nitro, dimethylamine, and isopropyl groups scored the lowest. Additionally, substituents in the 6 positions were observed to perform poorly. Visual analysis of these poor performers showed that they spend more time interacting with residues in the gorge and bottleneck areas on the side of the active site opposite the phosphonate.

Analysis of the diffusion of the three charge states of corriganine via the Tomodock program revealed that the ligands prefer to avoid the oxyanion hole portion of the active site. The ligands also move down toward the cation binding region where piperidine pi-pi interaction with the Trp_{86} residue is

highly conserved. There is a notable lack of the expected ligand interaction with the phosphonate, this may be because an additional gridbox centered behind the phosphonate was not included. Lowering the bottom gridbox center and increasing the number of gridboxes may remedy this problem in future simulations.

4.2 Future Work

In the search for a better realkylating compound studies such as this one which utilize computational methods to analyze a library of compounds for their affinity for the active site have shown their ability to predict molecules that have in vitro activity. This library yielded some promising ligands, namely 5-OH-corriganine, 5-NH_3-corriganine, 4-CH_2CH_3-corriganine, and 4-Cl-corriganine, that will be passed on to our collaborators to be synthesized and tested for activity.

Further analysis of these compounds in other charge states is warranted as the active site of AChE may alter the protonation of the ligand as it diffuses down the gorge and interacts with the active site. New ligands with strong electron donating groups should be investigated to find a ligand with better affinity for the active site. Additionally, computational analysis of more libraries of compounds with different substituents and substituent patterns on corriganine are a likely source of the next corriganine like ligand. Also, use of the Tomodock computational analysis technique may also serve to greater elucidate the manner in which ligands interact and diffuse down to the active site of AChE.